frontiers | Frontiers in Earth Science

TYPE Original Research
PUBLISHED 02 March 2023
DOI 10.3389/feart.2023.1140030

OPEN ACCESS

EDITED BY
Faming Huang,
Nanchang University, China

REVIEWED BY
Honggang Wu,
Northwest Research Institute Co., Ltd. of C.R.E.C, China
Yulong Cui,
Anhui University of Science and Technology, China
Min Lee Lee,
University of Nottingham Malaysia Campus, Malaysia

*CORRESPONDENCE
Jianhui Dong,
dongjianhui@cdu.edu.cn
mailto:dongjianhui@cdu.edu.cn

SPECIALTY SECTION
This article was submitted to Environmental Informatics and Remote Sensing, a section of the journal Frontiers in Earth Science

RECEIVED 08 January 2023
ACCEPTED 16 February 2023
PUBLISHED 02 March 2023

CITATION
Wu Y, Dong Y, Wei Z, Dong J, Peng L, Yan P and Ma W (2023), Genetic mechanisms and a stability evaluation of large landslides in Zhangjiawan, Qinghai Province.
Front. Earth Sci. 11:1140030.
doi: 10.3389/feart.2023.1140030

Genetic mechanisms and a stability evaluation of large landslides in Zhangjiawan, Qinghai Province

Yuanzao Wu[1,2,3], Yangdan Dong[4], Zhanxi Wei[1,2,3], Jianhui Dong[5,6]*, Liang Peng[7,8], Pan Yan[9] and Wenli Ma[1,2,3]

[1]Qinghai 906 Engineering Survey and Design Institute Co., Ltd., Xining, Qinghai, China, [2]Key Laboratory of Environmental Geology of Qinghai Province, Xining, Qinghai, China, [3]Qinghai Geological Environment Protection and Disaster Prevention Engineering Technology Research Province, Xining, Qinghai, China, [4]State Key Laboratory of Geological Disaster Prevention and Environmental Protection, Chengdu University of Technology, Chengdu, China, [5]Sichuan Engineering Research Center for Mechanical Properties and Engineering Technology of Unsaturated Soils, Chengdu, China, [6]School of Architecture and Civil Engineering, Chengdu University, Chengdu, China, [7]Qinghai Hydrogeology and Engineering Geology and Environgeology Survey Institute, Xining, China, [8]Hydrogeological and Geothermal Geological Key Laboratory of Qinghai Province, Xining, China, [9]Sichuan Changjiang Vocational College, Chengdu, China

It is important to study the instability law of typical landslides to understand the evolution of regional landslides and for disaster prevention. This study uses the Zhangjiawan landslide in Xining City, Qinghai Province, as an example. Through field surveys and an analysis of the geological environmental conditions, the formation and evolution mechanisms of the Zhangjiawan landslide are summarized. The stability of the Zhangjiawan landslide was evaluated using limit equilibrium and numerical simulation methods to provide theoretical support for the susceptibility of the Zhangjiawan landslide. The results show that the main reasons for the occurrence of multi-grade landslides are the steep and gentle terrain changes, the poor permeability of the mudstone lithology, the excavation of the front anti-slide section, and rainfall. The whole deformation and failure mechanism of the landslide is the "unloading rebound-tension deformation-creep deformation." The results of the numerical simulation and the limit equilibrium methods are nearly the same, and the difference in the stability coefficients is small. Under rainstorm conditions, the displacement and the maximum shear strain increments are mainly concentrated on the rear edge of the landslide mass, and the front edge is pushed, which is a typical push-type landslide.

KEYWORDS

Zhangjiawan landslide, stability evaluation, genetic mechanisms, numerical simulation, limit equilibrium method

1 Introduction

Since the middle of the 20th century and with the increase in the expansion of the scope of human engineering activities, more and more geological disasters have occurred. Landslides, which are a form of slope failure, are the most common geological disasters in the Xining area of Qinghai Province (Hu and Wei, 2008; Ma, 2015; Wei et al., 2015). Recently, related research on the Xining landslide resulted in extensive achievements. Zhao

(1994) studied the development characteristics of a loess landslide in Xining City and evaluated the stability of a typical Xiaoyoushan loess landslide. Liu and Sun (1994) analyzed the stability of the Xinyuan landslide under different working conditions using the transfer coefficient method. Yao et al. (2014) expounded on the deep causes of a landslide in Beishan, Xining, from the perspective of the geological structure. Shen et al. (2018) summarized the calculation and evaluation methods of various types of landslide stability. Zhang et al. (2020) analyzed the seepage characteristics and stability of old landslides under rainfall conditions using Studio software. Sun et al. (2020) classified the landslide in Xining City and used a weighted information volume model to evaluate the landslide susceptibility. Peng et al. (2021) studied the temporal and spatial, structural, and deformation characteristics as well as the formation mechanism of the Zhangjiawan landslide and conducted real-time automatic professional monitoring of the Xining landslide (Bai et al., 2021; Peng et al., 2021).

To minimize the threat to human life and property from landslides, a slope stability evaluation is particularly important. Nowadays, research studies on landslide stability analysis methods at home and abroad are relatively advanced. These methods can be summarized into three categories: the qualitative analysis method, the quantitative calculation method, and the uncertain analysis method. The qualitative analysis examines the main factors affecting the stability of a landslide after considering the engineering geological investigation, and the possible deformation failure mode and geomechanical mechanism of the slope are inferred. Thus, when combined with the deformation development characteristics of the slope, the current stage of the slope is judged, and a qualitative analysis of its stability is completed. This mainly includes graphic and engineering analogy methods (Zhou et al., 2008). This type of qualitative analysis requires a higher level of experience from evaluators and has certain regional limitations. Quantitative analysis is a method to calculate the stability coefficient and displacement deformation value of a landslide using the basic theories of rock mass mechanics and soil mechanics, and the stability of the slope according to the calculated eigenvalues is analyzed. Presently, there is mainly a limit equilibrium method and a numerical simulation method (Jiang et al., 2018). Due to its simplicity and efficiency, the limit equilibrium method is widely used in landslide stability calculations and mainly includes the Swedish strip, Janbu, Bishop, and transfer coefficient methods (Zhang and Zheng, 2004; Wang et al., 2014; Cheng et al., 2015; Wang et al., 2020; Wu et al., 2022). Numerical simulation is a multidisciplinary analysis method that combines mathematics, mechanics, and computer-aided research programs, which can simulate and analyze the stress, strain, and displacement of the geological environment of a landslide under the action of an external load. As early as 1966, the finite element method was used by American scholars to analyze the stability of a soil slope. Later, additional scholars added it to the numerical simulation of the landslide, and great development and improvement have been made (Zhang et al., 2003; Zhang et al., 2011; Shan et al., 2022). With the deepening of research on landslide stability, the dynamic and uncertain characteristics of landslide stability have gradually become reflected in engineering practice. Therefore, a new method adapted for landslide dynamic stability is proposed and includes a reliability analysis, a neural network, and random process and fuzzy mathematics methods (Jiang et al., 2000; Shalanov and Aletdinova, 2017; Huang et al., 2020; Menegoni et al., 2020).

Recently, many scholars have improved and perfected various stability evaluation methods. Wang et al. (2008) combined the strength reduction and limit analysis methods to obtain a calculation method of the landslide stability coefficient to examine the stability evaluation of a heterogeneous soil slope. Li et al. (2009) discussed the improvement of the strength reduction method compared with the limit equilibrium method in landslide stability analysis. Huang et al. (2013) proposed two- and three-dimensional rotation-translation mechanisms based on the upper bound theorem to study the stability of slopes with weak interlayers and pore water pressure. To obtain the stability state of a slope in the process of progressive failure, Chen et al. (2015) improved the strength reduction method and proposed a dynamic slope stability evaluation method. Zhou and Cheng (2015) proposed a new strict limit equilibrium method based on displacement to analyze the stability and displacement of the three-dimensional creep slope. Nian et al. (2016) proposed a stability evaluation method suitable for a multi-stage complex slope. Song (2017) proposed a method to analyze the surface stability of rain-induced landslides. Xiong et al. (2019) conducted a detailed description of the Green-Ampt model modification and the safety factor derivation process and completed the stability evaluation of a multi-layer slope under rainfall conditions. Tang et al. (2021) used SLOPE/W to evaluate the seepage stability of large landslides affected by reservoir water-level fluctuation and rainfall. Tong et al. (2021) evaluated the slope stability through fracture displacement and GPS data in the study area. Yao et al. (2021) combined a rainfall infiltration module in TRIGRS with Scoops3D to analyze the slope stability under extreme rainfall conditions. Ning et al. (2022) evaluated the stability of a large paleo landslide using the cusp mutation model.

To protect the property safety of the people in the residential area of the Zhangjiawan landslide front, this paper analyzes the formation and evolution mechanism of the Zhangjiawan landslide by combining the geological environment conditions of the landslide area with the field investigation data. The limit equilibrium and numerical simulation methods are used to evaluate the stability of the Zhangjiawan landslide in Qinghai Province.

2 Study area

2.1 Regional geological and environmental conditions

The study area is located in the transitional zone between the eastern end of the Qilian Middle Uplift Belt and the western part of the Lajishan Eugeosynclinal Belt in the Qilian Caledonian fold system. During the Tertiary Period, strong tectonic movements in the study area caused the descent of rock layers and the deposition of a huge thickness of lacustrine clastic rocks. During this period, other tectonic influences led to the formation of broad and gentle dipping and oblique structures in the basin with a predominantly north-west-south-east orientation. The fault and fold tectonic activity in the Xining Basin was relatively weak,

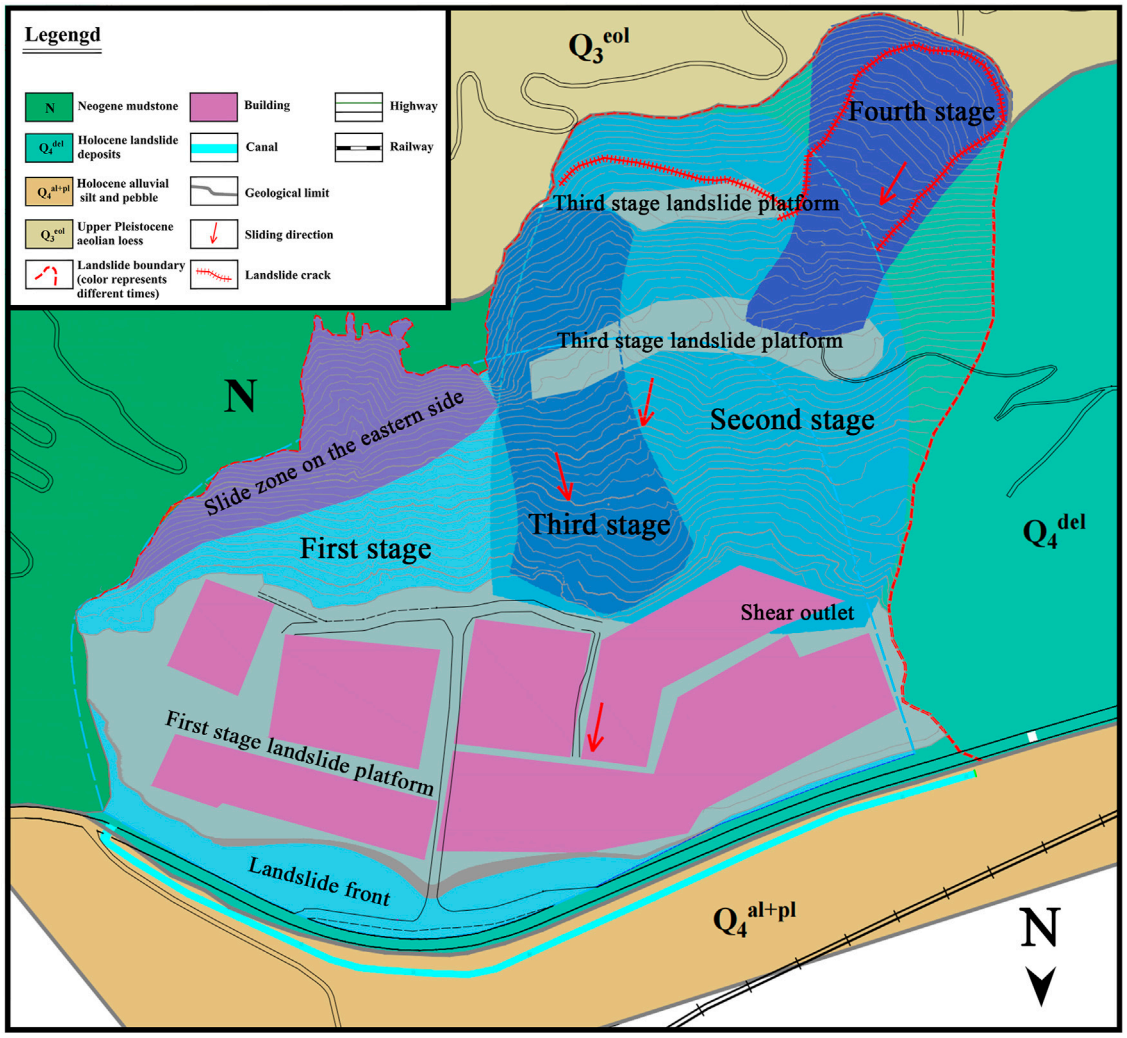

FIGURE 1
Engineering geological plan of the study area.

especially in the belly of the basin. However, the boundary fault activity was very strong, and the tectonic activity is mainly manifested in the overall uplift of the vertical movements.

The overall topography of the study area is higher in the south and lower in the north, with a relative height difference of 430 m. Based on geomorphology type and morphological characteristics, the study area was divided into two geomorphic units: the low mountain and hill area and the valley plain area (Figure 1). The low mountain and hilly areas are located to the south of the Huangshui River Valley with an altitude of more than 2,300 m. Its terrain is steep in the upper part and gentle in the lower part. Water flow erosion created a high and steep slope at the front edge, and the terrain is broken. The valley plain area is located in the valley area on the south bank of the Huangshui River, with an altitude of 2,200 ~ 2,450 m and a valley width of 3 ~ 4 km. The terrain is relatively open and flat; it is high in the west, low in the east, high in the south, low in the north, and slightly inclined to the riverside.

The pre-Quaternary strata exposed in the study area were mainly Neogene mudstone and sandstone interbeds (N1), see Figure 2. This layer was the main stratum in the study area, the basement of the valley area, and the main body of the low mountains and hills. It consists of a brick-red mudstone and a purplish-red sandstone and was mainly exposed in the middle and upper parts of the high and steep slopes at the front edge of the low mountains and hill area. The intensely weathered thickness of the rock stratum was generally 5 ~ 8 m, and the occurrence was 335°∠3° (Figure 3). The surface lithology was strongly weathered, and the joint fissure was abundant. There were three groups of joints in the stratum with a strike of 30° ~ 60° and 270° ~ 290° and nearly in the north-south direction, and the dip angle was 85°. The completely weathered mudstone constituted the main easy-sliding stratum in the study area.

The study area belongs to the plateau continental semi-arid climate. The temperature difference is significant, the precipitation is light but concentrated, and the evaporation is heavy. The average annual temperature in the Xining area is 6.1 °C, and the annual temperature difference is 24.7 °C. The distribution of the precipitation is uneven and generally

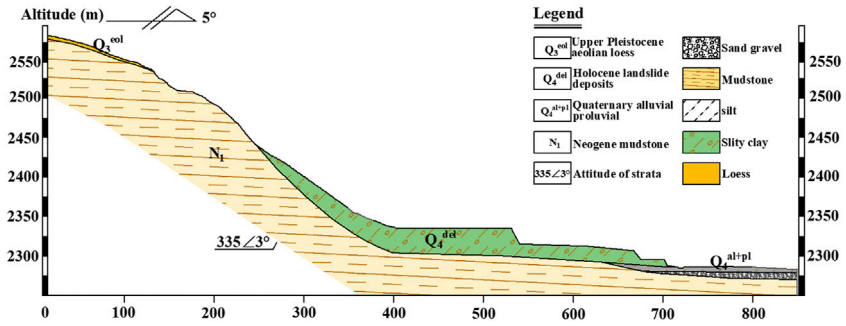

FIGURE 2
Schematic diagram of a typical engineering geological section.

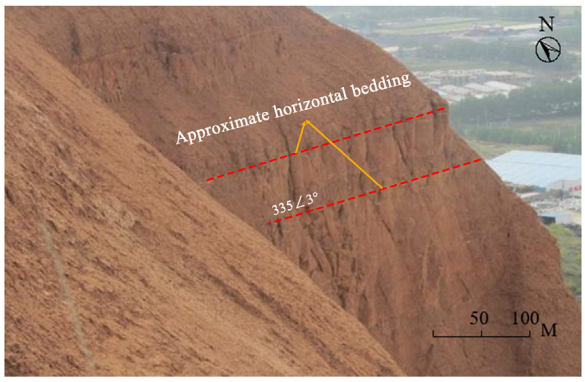

FIGURE 3
Near-horizontal mudstone beddings.

concentrated in the summer. The annual precipitation is obviously altered.

2.2 Basic characteristics of landslides

The Zhangjiawan landslide is located south of the Haihu Steel Market in Zhangjiawan Village. The southern part of the landslide is in a low-mountain and hilly area. The rear wall of the landslide is in the shape of a steep cliff. The boundary extends from the shear outlet of the front edge to the Jiefang Canal. The elevation of the rear edge of the landslide is 2,620 m, and that of the toe of the front edge is 2,295 m. The slope height is 325 m, and the average gradient is 30°. The formation mechanism of the Zhangjiawan landslide was quite complicated. According to the characteristics of the landslide shape, sliding surface, shear outlet, and sliding nappe, landslides can be divided into four stages of graded sliding and three levels of platforms (Figure 4). The plane shape was an irregular "tongue shape," and the profile shape was concave. There were three levels of ladder platforms, which were formed by the repeated sliding of the landslide. The landslide is 400–1,100 m long from north to south and 200–600 m wide from east to west. It is a very large landslide and belongs to a compound landslide of gently inclined, layered rock and soil.

2.3 Deformation and failure characteristics of the landslide

The Zhangjiawan landslide mainly consists of tensile deformation and ground displacement. The tensile deformation is mainly concentrated in the middle and rear parts of the landslide. Shear cracks are located at the boundary of the landslide, which is generally distributed in the exploratory well. Swelling and cracking of the retaining wall caused by foundation settlement often occurred on the front edge of the high and steep slopes, and the deformation of the buildings is mainly distributed in the steel market in the middle and lower parts of the landslide.

2.3.1 Tensile cracks

The rear edge tensile crack deformation mainly occurred in the rear wall zone of the west side slope of the Zhangjiawan landslide, which was where tensile cracks and landslide depression developed. Tensile cracks generally developed (Figure 5) with a crack strike of 300°–320° and an extension length of 40–102 m. These cracks run approximately parallel to the rear edge slope; their width approximately ranges from 0.10 and 1.2 m, and their maximum depth reaches 1.8 m. In addition, the trees on it were askew, and the soil body was messy. The crack surface is rough and uneven, and its filling material is mainly mud.

2.3.2 Shear and bulging cracks

The shear crack (Figure 6) was found at the SK No. 1 test pit on the east boundary of H1-2. The crack struck at 22° and was 0.05–0.25 m wide. The upper part of the crack was straight, and the lower part was slightly tortuous. The filling was muddy with a small amount of gravel. The exposure depth was 3.5 m. In test pit SK2 (Figure 7) at the side of the second-stage sliding slope platform in the middle of H1-2, obvious shear cracks also occurred. These cracks were mainly surface shear cracks with a crack strike of 32° and a width of 0.01–0.05 m. The cracks were relatively straight, and there were few fillings and muddy fillings with an exposure depth of 3.0 m.

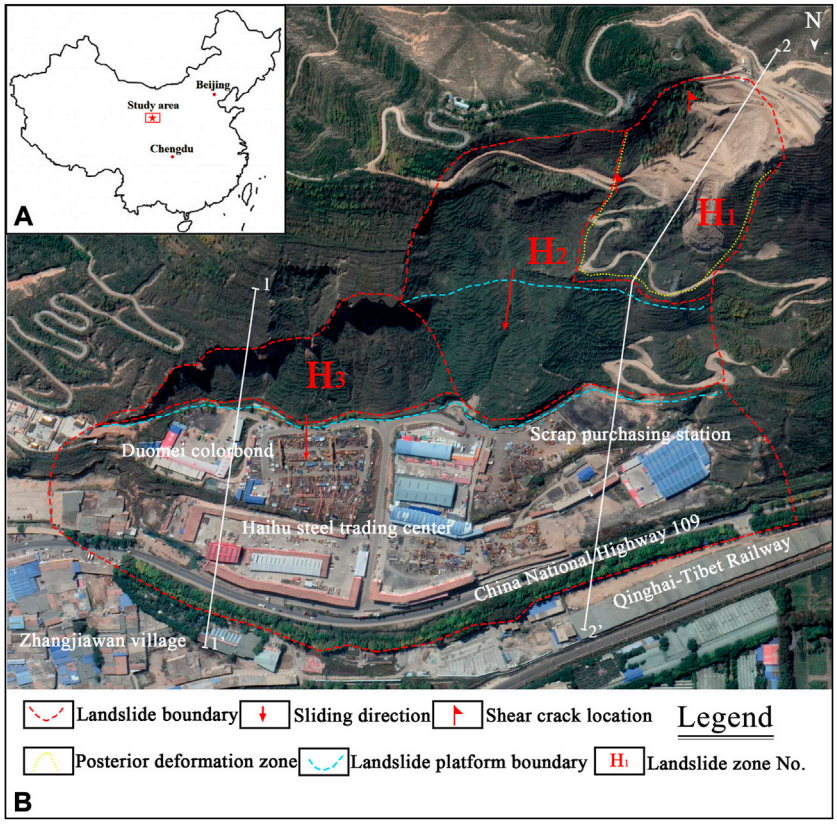

FIGURE 4
(A) Map of the geographical location of the study area and **(B)** plane morphological characteristics of the Zhangjiawan landslide.

FIGURE 5
Tensile crack on the west side of the landslide's rear edge.

FIGURE 6
H1-2 east boundary shear crack (SK1).

The bulging cracks were generally located at the middle of the front edge of the landslide. These cracks were only visible in the local section, with an extension direction of 0.5–1.1 m, a strike of 215°–305°, and a width of 0.02–0.10 m. Due to the extrusion and uplift of the lower part of the landslide mass caused by sliding obstruction, bulging cracks in the vertical sliding direction were formed. The retaining wall on the south side of the G109 National Highway at the front edge of the landslide experienced bulging deformation due to a creep of the Zhangjiawan landslide. The bulging height was approximately 1 cm and bulging cracks could

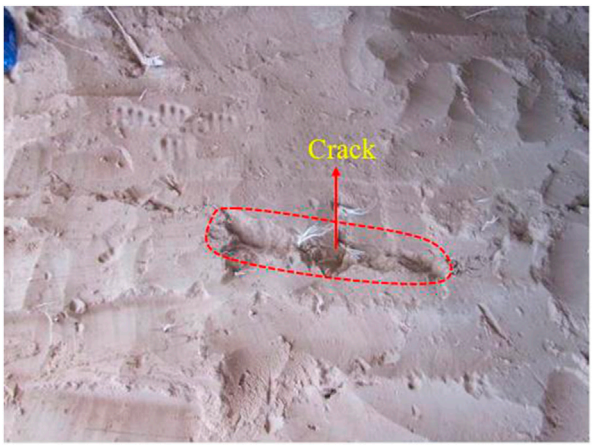

FIGURE 7
H1-2 lateral shear cracks on the middle second-stage landslide platform (SK2).

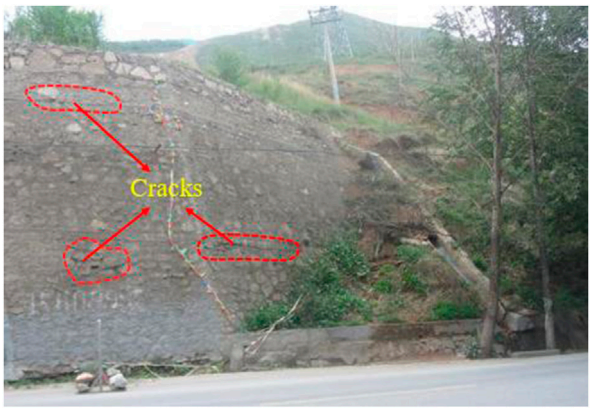

FIGURE 8
Crack development on the retaining wall.

be generally observed (Figure 8). The trend was mostly near the horizontal and vertical directions. The crack length was 1~5 m, the width was 2 ~ 5 mm, and the original retaining wall was approximately 12 ~ 15 m high.

3 Methods

3.1 Limit equilibrium method

The limit equilibrium method assumes that the sliding surface and rock mass are rigid plastic bodies. The rock and soil mass within the sliding range is divided into strips, the equilibrium equation is established, and the stability coefficient of the slope is calculated. In this study, the transfer coefficient and residual sliding force methods are used to analyze the stability of the landslide. The transfer coefficient method can obtain the stability coefficient and residual sliding force of the sliding body, and the calculation is accurate and applicable. The characteristics of the transfer coefficient method are as follows: the whole sliding body obeys the force balance along the sliding surface but does not obey the moment balance; the sliding surface failure follows the Mohr–Coulomb criterion. The stress on the sliding surface is shear stress parallel to the sliding surface and normal stress perpendicular to the sliding surface. As a rigid body, the sliding body does not deform in the sliding process. As long as the shear strength of the sliding surface is not enough to resist the shear force generated by the sliding body, the sliding body will slide along the sliding surface, and the direction of the residual sliding force of the strip is consistent with the direction of the sliding surface. Figure 9 shows a schematic diagram of soil blocks and the stress calculation in the process of the transfer coefficient method, and the stability coefficient is calculated using Eqs 1–11.

$$K_s = \frac{\sum_{i=1}^{n-1}\left(R_i \prod_{j}^{n-1} \varphi_j\right) + R_n}{\sum_{i=1}^{n-1}\left(T_i \prod_{j=i}^{n-1} \varphi_j\right) + T_n}, \tag{1}$$

$$R_n = (W_n(1 - r_u)\cos\alpha_n - A\sin\alpha_n) - R_{Dn})\tan\varphi_n + c_n L_n, \tag{2}$$

$$T_n = W_n(A\cos\alpha_n + \sin\alpha_n) + T_{Dn},$$

$$\prod_{j=i}^{n-1} \varphi_j = \varphi_i \varphi_{i+1} \varphi_{i+2} \cdots \varphi_{n-1}, \tag{3}$$

$$N_{W_i} = \gamma_W h_{i_W} L_i. \tag{4}$$

Division of the penetration pressure parallel to the slip surface:

$$T_{D_i} = \gamma_W h_{i_W} L_i \tan\beta_i \cos(\alpha_i - \beta_i). \tag{5}$$

Penetration pressure vertical slip surface component:

$$R_{D_i} = \gamma_W h_{i_W} L_i \tan\beta_i \sin(\alpha_i - \beta_i). \tag{6}$$

In the formula, φ_j is the transfer coefficient (j = i) for the transfer of the remaining slip force from block i to block i + 1, which indicates

$$\varphi_j = \cos(\alpha_i - \alpha_{i+1}) - \sin(\alpha_i - \alpha_{i+1})\tan\varphi_{i+1}, \tag{7}$$

$$T_i = W_i \sin\alpha_i + P_{wi}\cos(\theta_i - \alpha_i) + Q_i \cos\alpha_i, \tag{8}$$

$$R_i = N_i \tan\varphi_i + c_i L_i, \tag{9}$$

$$N_i = W_i \cos\alpha_i + P_{wi}\sin(\theta_i - \alpha_i) + Q_i \sin\theta_i, \tag{10}$$

$$E_i = E_{i-1}\varphi + KT_i - R_i, \tag{11}$$

where K_s is the stability factor; W_i is the gravity of the i-block, the natural gravity is considered on the infiltration line, and the saturation gravity is considered below the infiltration line (kN); θ_i is the angle between the gravity line of the i-block and the radius of the midpoint through the bottom surface of this block (°); α_i is the sliding surface inclination of the i-block (°); β_i is the angle between the groundwater flow line and the slip surface in the i-block (°); L_i is the length of the sliding surface of the i-block (m); c_i is the effective cohesive force on the slip surface of the i-block (kPa); φ_i is the effective internal friction angle of the sliding surface of the i-block (°); E_i is the remaining sliding force of the ith sliding body (kN); E_{i-1} is the remaining sliding force of the (i-1) sliding body (kN); φ_j is the transmission coefficient; Q_i is the horizontal force of the i-block (kN); K is the safety factor; and A is the earthquake acceleration (gravitational acceleration g).

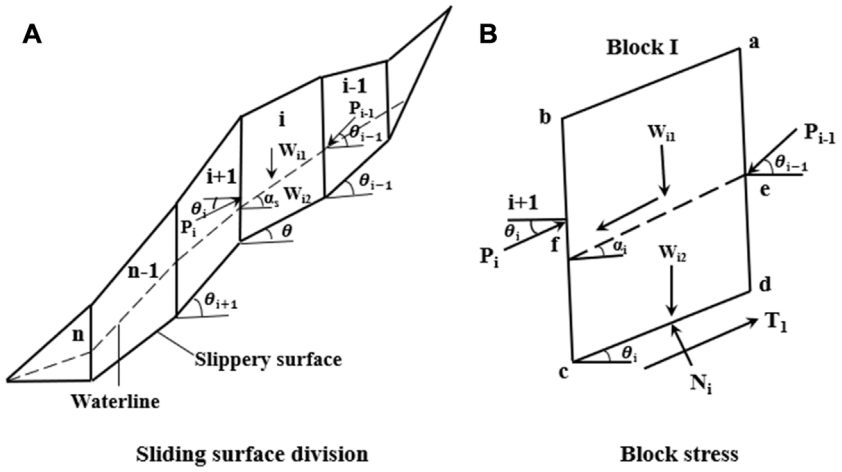

FIGURE 9
Transfer coefficient method calculation diagram: **(A)** sliding surface division and **(B)** block force.

3.2 Principles for solving slope stability (FLAC)

FLAC finite difference software is a numerical simulation software developed by ITASCA in the United States that has a wide range of simulation fields and more powerful computing power. A finite difference method is used to transform the solution of the differential equation into an algebraic equation. FLAC contains a variety of constitutive models, and the Mohr–Coulomb ideal elastoplastic model is commonly used in the geotechnical engineering field. When the software is used for the analysis and calculation, the written command flow file is imported into the software, and the software is run under the control of the command flow file.

3.2.1 Strength reduction principle of the finite element

The slope stability analysis' finite element strength reduction method continuously reduces the shear strength parameters of the slope's rock and soil mass until it reaches the ultimate failure state. The program automatically obtains a sliding failure surface based on the elastic–plastic finite element calculation results, in addition to the strength reserve safety factor of the slope. As this method is very close to an engineering design, slope stability analysis will certainly enter a new era. For the Mohr–Coulomb materials, the safety factor of the strength reduction can be expressed as

$$\tau = \frac{c + \sigma \tan \varphi}{\omega} = \frac{c}{\omega} + \sigma \frac{\tan \varphi}{\omega} = c' + \sigma \tan \varphi'. \quad (12)$$

So there are

$$c' = \frac{c}{\omega}, \quad \tan \varphi' = \frac{\tan \varphi}{\omega}. \quad (13)$$

The definition of this strength reduction safety factor is consistent with the definition of the safety factor of the limit equilibrium strip method of slope stability analysis, and both belong to the strength reserve safety factor; however, for the actual slope engineering, they all represent the safety factor of the entire sliding surface, i.e., the average safety factor of the sliding surface rather than the safety factor of a certain stress point. The algorithm is built into the FLAC software.

3.3 Stability evaluation criteria

According to the Code for Landslide Prevention and Control Engineering Survey, the stability state of a landslide can be divided according to the stability coefficient. When the stability coefficient Fs is less than 1.00, the landslide is unstable. When the stability coefficient Fs is between 1 and 1.05, the landslide is in an unstable state. When the stability coefficient Fs is between 1.05 and 1.15, the landslide is in the basic stable state. When the landslide stability coefficient Fs is greater than 1.15, the landslide is in a stable state.

4 Results and discussion

4.1 Mechanisms and evolution of the Zhangjiawan landslide

4.1.1 Analysis of the formation mechanisms

The ancient Zhangjiawan landslide is a typical push-type landslide, which developed on the slope at the junction of the hilly and alluvial plain areas on the south bank of the Huangshui River. It is an unfavorable geological complex with multiple multi-level landslides and collapses on the back and side walls of the old landslide. Landslides and the resulting collapse easily occur in the transition area between the Huangshui River Valley and the low mountain and hill areas. The terrain in the study area is steep, and the free surface provides good terrain conditions for the landslide. The lithology of the original slope in the study area is made of Neogene mudstone, which has poor permeability. The catchment water at the pass and the slope surface was softened

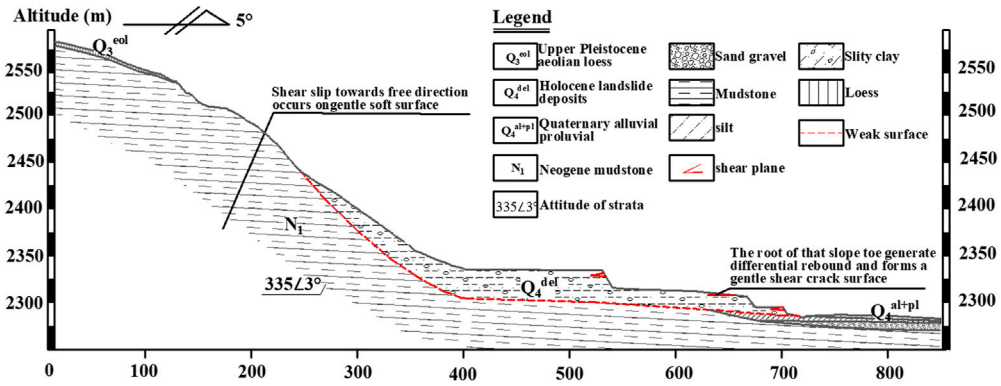

FIGURE 10
Unloading rebound stage.

and argillated due to the influence of mudstone surface water resistance, which resulted in a weak sliding zone. The two reasons mentioned previously were the main reasons that the old landslide was induced. After the old landslide, a high and steep back wall of the landslide was formed, exposing nearly vertical Neogene mudstone and Malan loess. Therefore, the landform and lithology conditions in the study area are the main reasons for the formation of the landslide.

The most direct reason for the resurgence of the ancient Zhangjiawan landslide is human activities. A large number of human engineering activities excavated and leveled the anti-sliding section of the front edge of the old Zhangjiawan landslide mass in different periods and degrees. This changed the original natural and stable state of the landslide mass. After the front edge excavation and slope stress redistribution, stress concentration and large deformation occurred in the middle and rear parts.

Second, the rainstorms in the study area are mostly concentrated in the summer, with an annual average rainfall of 414.5 mm. The study area is one of the areas with the highest rainfall intensity in the whole province. The maximum precipitation amounts in 1 hour and 24 hours were 32 mm and 66 mm, respectively, which are precipitation conditions that may cause landslides (Huang et al., 2022). The rainfall infiltration increased the gravity of the surface rock and soil mass, soaked the potential sliding surface, reduced sliding resistance, and induced the landslide. This is also the main factor in a landslide.

4.1.2 Deformation mechanism analysis

The slope in the study area is steep in the upper part and gentle in the lower part, with an upper slope greater than 45°. It belonged to the gentle layered rock and soil composite slope. After front edge stress redistribution was induced by a manual excavation of the slope toe, the slope body produced a slow creep, sliding along the gentle layer surface toward the direction facing the void in front of the slope. Therefore, it was determined that the mechanical deformation mechanism and failure are slipping-pressing tensile cracking. The deformation process is divided into the following three stages:

4.1.2.1 The unloading rebound stage

This stage occurred during the manual excavation of the slope toe. In the early excavation stage, a differential rebound occurred above and below the restricted surface at the root of the slope toe. Due to the existence of a flat, weak surface, the slope body produces a flat, shear-cracked surface at the slope toe. During excavation, shear sliding occurred along the flat, weak surface toward the air direction, and the sliding speed was relatively slow, as shown in Figure 10.

4.1.2.2 The tensile deformation stage

After a period of manual excavation of the slope toe and with the development of deformation, the shear crack extended to the ground. The rock and soil structures on the slope became loose with the development of deformation. The tension crack occurred nearly vertically to the slip plane and was produced around the locking point of the slip plane due to the concentration of tensile stress, and the tensile crack extended upward and generally parallel to the slope surface gradually and was accompanied by a local slip (Figure 11).

4.1.2.3 The creep deformation stage

When the treatment was not conducted in time in the tensile cracking deformation stage, the deformation entered a cumulative destruction stage. During this stage, the deformation body rotated, and the chimeras at the steep and gentle junction were crushed and sheared one by one, accompanied by a dilatancy phenomenon. Thus, the slope surface was slightly uplifted and the rock and soil body slid along the weak surface. The rock stratum layer showed obvious argillization signs, and clear slope scratch marks were observed on an argillization film. This observation indicated that the creep deformation stage was in progress. The landslide occurs when the steep fracture surface and the gentle slip surface develop into a through slip surface, as shown in Figure 12.

4.2 Stability analysis of the Zhangjiawan landslide

In this section, limit equilibrium and numerical simulation methods are adopted to quantitatively analyze the stability of the

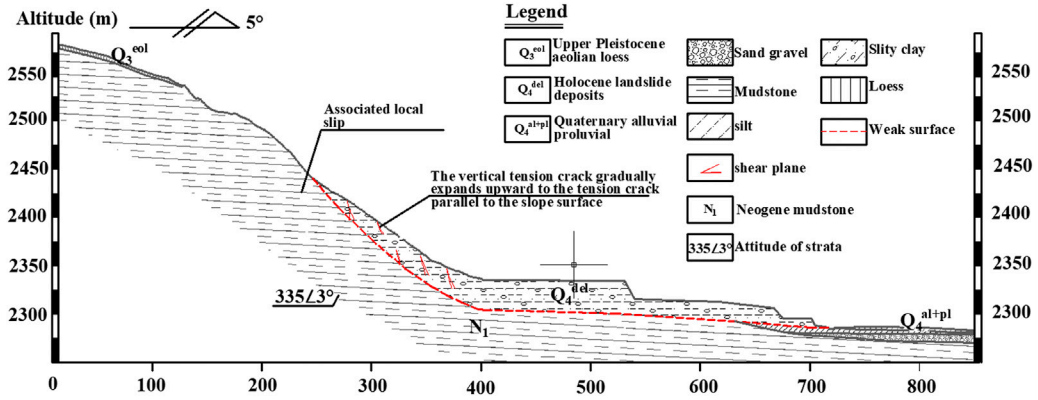

FIGURE 11
Tensile deformation stage.

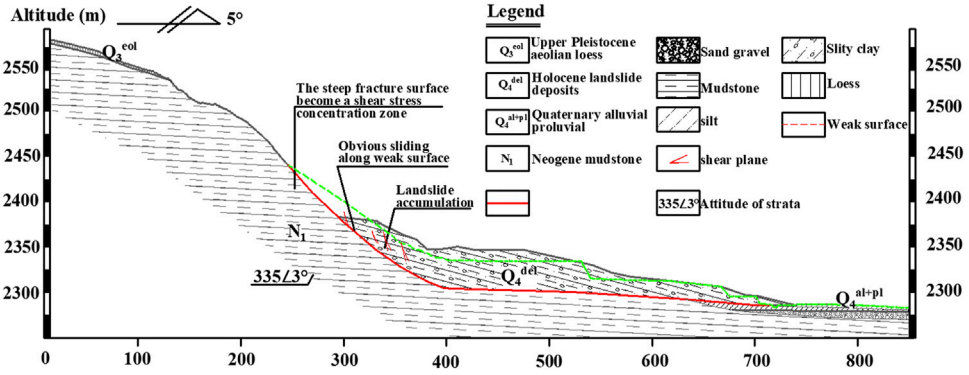

FIGURE 12
Creep deformation stage.

Zhangjiawan landslide. The limit equilibrium method is the most commonly used current method in engineering practice. Its principle is to analyze the static balance of unstable rock and soil masses on the slope and evaluate the slope's stability through the relationship between the anti-sliding force and sliding force. Because the limit equilibrium method considers the sliding soil body as a rigid body, it ignores the influence of the deformation of the sliding body itself. Hence, this paper combines the numerical simulation method, analyzes the stress–strain characteristics of the sliding body, and evaluates the stability of the landslide using the finite element strength reduction method. The calculation results of the limit equilibrium method are verified.

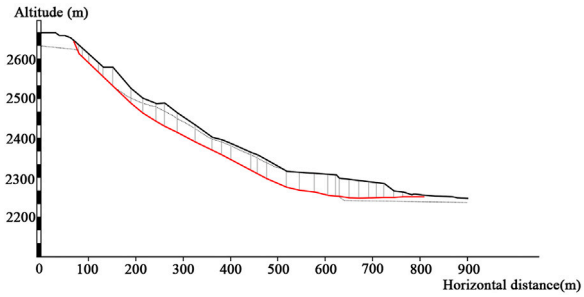

FIGURE 13
Calculation diagram of the 1-1′ section stability.

4.2.1 Limit equilibrium analysis

4.2.1.1 Establishment of a computational model

According to the survey, the sliding surface (zone) of the Zhangjiawan landslide is similar to a broken line type. Therefore, according to the Code for the Survey of Landslide Prevention and Control Engineering, the transfer coefficient method is adopted. The 1-1′ and 2-2′ sections are selected as the calculation sections (Figures 13, 14) to calculate the stability of the Zhangjiawan landslide under natural and rainstorm conditions.

The calculation parameters are comprehensively determined according to an indoor test on rock and soil samples taken from boreholes. In this paper, the mechanism of the landslide is

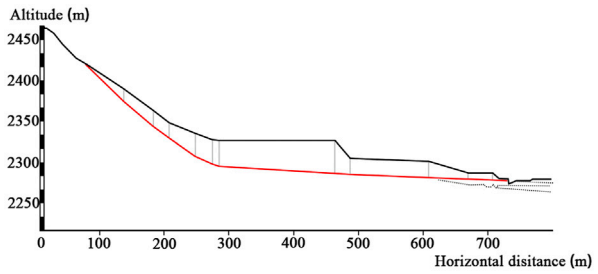

FIGURE 14
Calculation diagram of the 2-2′ section stability.

analyzed, and the back-calculation is conducted according to the different sliding zone properties of loess-like soil and silty clay and the difference in the parameters in different parts of the same section. After a thorough analysis, the back-calculated index is seen as the mechanical design parameter for landslide control design. The comparison between the test results and the back-calculated results is shown in Table 1.

4.2.1.2 Limit equilibrium calculations

According to the calculation method, model, and parameters determined previously, the stability of the landslide under natural and rainstorm conditions is calculated. The calculations of the stability coefficient of the landslide are listed in Table 2.

Through the stability calculation, the stability coefficients of 1-1′ and 2-2′ sections of the landslide under the natural state are 1.14 and 1.11, respectively. Both coefficients are greater than 1.05 and less than 1.15, and they are basically in a stable state. However, the stability coefficients of 1-1′ and 2-2′ sections of the landslide under the rainstorm state are 1.01 and 1.04, respectively. These two coefficients are less than 1.05 and greater than 1.0 and are in a less stable state.

4.2.2 Numerical simulation analysis and evaluation

4.2.2.1 Model building

Taking the Zhangjiawan landslide's representative sections 1-1′ and 2-2′ as the calculation sections, the finite difference numerical simulation analysis software is used for the model establishment and to calculate the slope stability under natural and rainstorm conditions.

The Mohr–Coulomb elastic-plastic constitutive model was selected in this study. The physical and mechanical parameters of the soil body obtained from indoor tests on rock and soil sampling at the landslide site are used as the simulation calculation parameters (Tables 3, 4). The horizontal velocity is imposed on the left and right sides of the constraint model. The bottom of the model is a fixed boundary, and the gravity stress field is a stress field.

4.2.2.2 Numerical simulation analysis

According to the simulation calculation method, model, and the aforementioned parameters, the stability of the landslide under natural and rainstorm conditions is calculated. The calculations of the landslide stability coefficient are shown in Table 5.

According to the aforementioned stability calculations, the representative sections of Phase I and Phase II Zhangjiawan landslides are basically stable under natural conditions. In contrast, under rainstorm conditions, the stability of the landslide is threatened and is in an unstable state. Therefore, the deformation and failure modes of the Zhangjiawan landslide are thoroughly analyzed in combination with the maximum shear strain increment diagram and displacement nephogram under rainstorm conditions. Figure 15 presents the simulation results of the 1-1′ and 2-2′ sections.

Figure 15 shows that, under the action of rainfall, the displacement is mainly concentrated at the rear edge of the landslide mass. The maximum displacement of the 1-1′ section is 0.48 m, and the maximum displacement of the 2-2′ section is 0.44 m. These displacements decrease gradually from the rear edge to the front edge, which indicates that the upper part of the landslide undergoes a large displacement and has an obvious pushing effect on the front edge.

TABLE 1 Comparison of the physical and mechanical indices of the sliding zone soil.

Working condition	Weight (γ) kN/m^3	Back-calculation indicator		Laboratory test result		Combined value	
		Cohesion (C) (Kpa)	Angle of internal friction (φ)	Cohesion (C) (Kpa)	Angle of internal friction (φ)	Cohesion (C) (Kpa)	Angle of internal friction (φ)
Natural	18.8	25.3	18°	25.9	23.2°	25.3	18°
Saturated	20.7	24.7	16°	23.2	18.3°	24.7	16°

TABLE 2 Calculations of the landslide stability coefficient (limit equilibrium method).

Calculated profile	Working conditions	Stability factor (Fs)	Stable state
1-1′	Natural working conditions	1.14	Basic stability
	Rainstorm conditions	1.01	Less stable
2-2′	Natural working conditions	1.11	Basic stability
	Rainstorm conditions	1.04	Less stable

TABLE 3 Physical and mechanical parameters of rock and soil masses in the natural state.

Rock	Cohesive force (Kpa)	Angle of internal friction (°)	Bulk modulus (Mpa)	Shear modulus (Mpa)	Density (g/cm^3)
Sliding body	28.0	26.1	6,400	3,800	3.26
Sliding bed	70	31.5	12,400	6,800	3.13
Slip tape	25.9	23.2	12,420	6,600	3.15

TABLE 4 Physical and mechanical parameters of rock and soil masses under rainstorm conditions.

Rock	Cohesive force (Kpa)	Angle of internal friction (°)	Bulk modulus (Mpa)	Shear modulus (Mpa)	Density (g/cm^3)
Sliding body	23.2	18.3	6,400	3,800	2.61
Sliding bed	40	30	12,400	6,800	2.50
Slip tape	23.2	18.3	12,420	6,600	2.51

TABLE 5 Calculations of the landslide stability coefficient (FLAC calculation).

Calculated profile	Working conditions	Stability factor (Fs)	Stable state
1-1′	Natural working conditions	1.11	Basic stability
	Rainstorm working conditions	1.02	Less stable
2-2′	Natural working conditions	1.12	Basic stability
	Rainstorm working conditions	1.04	Less stable

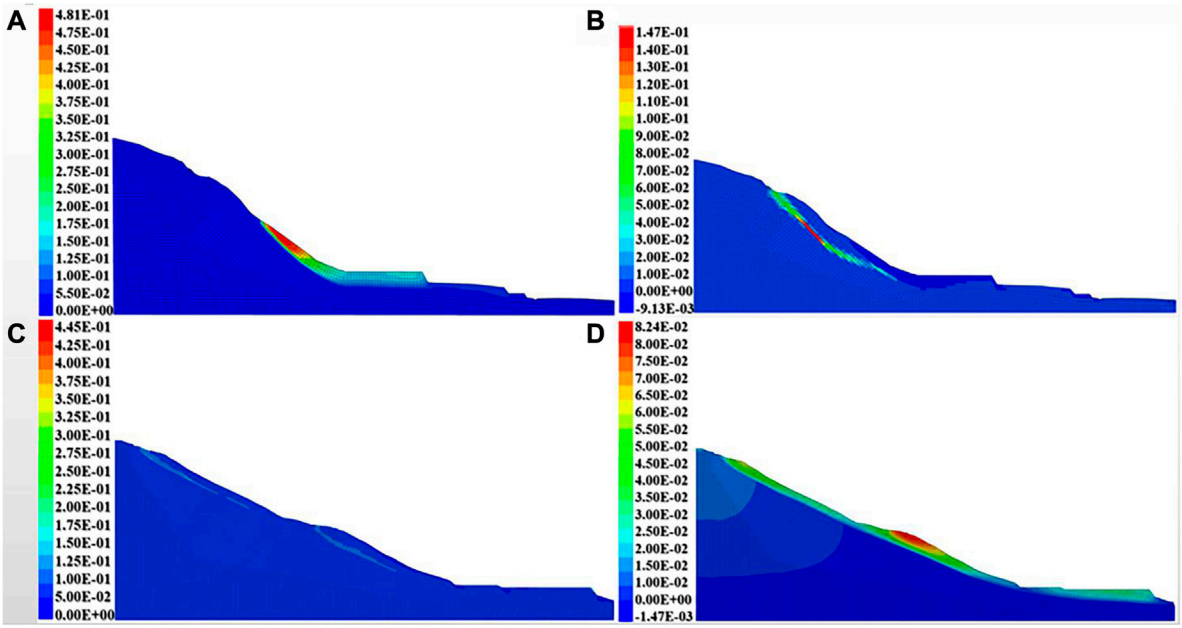

FIGURE 15
(A) Total displacement cloud of section 1-1′ (unit: m); **(B)** maximum shear strain increment of section 1-1′; **(C)** total displacement cloud of section 2-2′; and **(D)** maximum shear strain increment of section 2-2′.

In the numerical simulation, the landslide's maximum shear strain increment can reflect the range of shear deformation in the landslide mass. It is also the position of the potential sliding surface. The results show that the shear strain increment area of the two profiles is mainly distributed on the rear edge of the landslide and that the maximum value appears in the middle and rear of the

contact between the landslide mass and the bedrock. This indicates that the rear edge of the landslide is prone to a shear failure in the large-scale mode, which is caused by the increase in self-weight of the landslide mass and the decrease in soil strength in the sliding zone under rainstorm conditions. Shear failure occurs in the sliding zone soil in the deep part of the slope body. The shear failure area gradually penetrates and extends to the whole landslide, which belongs to a typical push-type landslide. Meanwhile, the landslide is in an unstable state. Without treatment, global sliding may occur in the shear failure area.

5 Conclusion

The study area is in an area with steep and gentle terrain change with a mudstone lithology with poor permeability. The excavation of the front anti-slide section and rainfall are the main reasons for the occurrence of multiple multi-level landslides. Landslides are considered a push-type sliding slope, and the landslide's whole deformation and failure process includes the unloading rebound stage, tensile deformation stage, and creep deformation stage. Shear failure occurs in the deep sliding zone of the slope and gradually extends to the whole sliding slope.

Data availability statement

The original contributions presented in this study are included in the article/Supplementary Material, and further inquiries can be directed to the corresponding author.

Author contributions

Writing—original draft preparation, YW; writing—review and editing, YD; resources, ZW; supervision, JD; methodology, LP; visualization, PY; investigation, WM. All authors have read and agreed to the published version of this manuscript.

Funding

The research in this manuscript was funded by the National Natural Science Foundation of China (Grant No. 41877273) and the Science and Technology Plan Project of Sichuan Province (Grant No. 2021YJ0053).

Conflict of interest

Authors YW, ZW, and WM were employed by Qinghai 906 Engineering Survey and Design Institute Co., Ltd.

The remaining authors declare that the research was conducted in the absence of any commercial or financial relationships that could be construed as a potential conflict of interest.

Publisher's note

References

Bai, Z. N., Peng, L., Shen, Y., and Zheng, C. Y. (2021). Characteristics and mechanism of the Zhangjiawan mega-landslide in. *Xining. Sci. Technol. Eng.* 21 (03), 927–934.

Cheng, J. Z., Wang, X. Q., Du, W. X., and Shi, H. L. (2015). Application of Janbu method in slope stability analysis of bayan obo mine. *Coal. Technol.* 34 (01), 130–132. doi:10.13301/j.cnki.ct.2015.01.046

Hu, G. S., and Wei, G. (2008). Basic types and distribution characteristics of extra-large landslides in Qinghai province. *Qinghai. Lnd. R. Mg.t Stgy* 06, 40–43.

Huang, F. M., Chen, J. W., LiuHuang, W. P. J., Hong, H., and Chen, W. (2022). Regional rainfall-induced landslide hazard warning based on landslide susceptibility mapping and a critical rainfall threshold. *Geomorphology* 408, 108236. doi:10.1016/j.geomorph.2022.108236

Huang, F. M., Jing, Z., Zhou, C. B., Wang, Y. H., Huang, J. S., and Zhu, L. (2020). A deep learning algorithm using a fully connected sparse autoencoder neural network for landslide susceptibility prediction. *Landslides* 17 (01), 217–229. doi:10.1007/s10346-019-01274-9

Huang, M., Wang, H., Sheng, D., and Liu, Y. (2013). Rotational-translational mechanism for the upper bound stability analysis of slopes with weak interlayer. *Comput. Geotech.* 53, 133–141. doi:10.1016/j.compgeo.2013.05.007

Jiang, L. W., Wang, S. T., Liu, H. C., and Han, K. L. (2000). Neural network evaluation of landslide stability in Wenchuan Jiaochang Section of Upper Minjiang River and analysis of river blocking possibility. *J. Mt. Sci-engl.* (06), 547–553. doi:10.16089/j.cnki.1008-2786.2000.06.012

Jiang, S. H., Huang, J., Huang, F. M., Yang, J. H., Yao, C., and Zhou, C. B. (2018). Modelling of spatial variability of soil undrained shear strength by conditional random fields for slope reliability analysis. *Appl. Math. Model.* 63, 374–389. doi:10.1016/j.apm.2018.06.030

Li, S. H., Liu, T. P., and Liu, X. Y. (2009). Analysis method of landslide stability. *Chin. J. Rock. Mech. Eng.* 28 (S2), 3309–3324.

Liu, H. X., and Sun, G. R. (1994). Geological hazards and geological environment in xining area. *Qinghai. Environ.* (01), 18–22.

Ma, H. Y. (2015). Study on the development characteristics of landslide geological hazards in nanchuan east road, xining city. *West. Chin. Sci-Technol.* 14 (06), 44–45.

Menegoni, N., Giordan, D., and Perotti, C. (2020). Reliability and uncertainties of the analysis of an unstable rock slope performed on RPAS digital outcrop models: The case of the gallivaggio landslide (western alps, Italy). *Remote Sens.* 12 (10), 1635. doi:10.3390/rs12101635

Nian, T. K., Liu, K., Huang, R. Q., Wang, L., and Zhang, Y. J. (2016). General upper limit method for stability of multi-stage multilayer complex slope. *Rock. Soil. Mech.* 37 (03), 842–849. doi:10.16285/j.rsm.2016.03.029

Ning, B., Liu, Y. J., and Wang, A. D. (2022). Stability evaluation and development trend analysis of giant pale landslides. *Geod. Geodyn.* 42 (05), 515–519. doi:10.14075/j.jgg.2022.05.014

Peng, L., Du, W., and Tian, H. (2021). Demonstration of monitoring and early warning of mega-landslides in. *Xining. Sci. Technol. Eng.* 21 (18), 7806–7813.

Shalanov, N. V., and Aletdinova, A. A. (2017). The relationship of categories of "risk" and "stability" of the non-stationary random process. *J. Phys. Conf. Ser.* 803 (1), 012138. doi:10.1088/1742-6596/803/1/012138

Shan, Z. G., Gao, S., Sun, M. J., Chen, Y. X., Li, L. P., Cheng, S., et al. (2022). Model test and numerical simulation of offshore landslide mechanism under wave action. *J. Rock. Soil. Mech.* 43 (S2), 541–552. doi:10.16285/j.rsm.2021.1835

Shen, Y. X., Yuan, S. X., Ma, M., and Tian, G. Z. (2018). Analysis on the formation mechanism of landslide disaster in xining city and its surrounding areas. *Qinghai. Land. Econ.* 04, 63–66. doi:10.13901/j.cnki.qhwxxbzk.2020.01.014

Song, E. Z. (2017). Prediction of shallow landslide by surficial stability analysis considering rainfall infiltration. *Eng. Geol.* 231, 126–138. doi:10.1016/j.enggeo.2017.10.018

Sun, C. M., Ma, R. Y., Shang, H. X., Xie, W. B., Li, Y., Liu, Y., et al. (2020). Evaluation of landslide susceptibility in Xining City based on landslide classification. *Hydrogeol. Eng. Geol.* 47 (03), 173–181. doi:10.16030/j.cnki.issn.1000-3665.201906074

Tang, J. F., Tang, X. M., Xiao, P., Wang, H., and Li, J. W. (2021). Analysis of seepage stability of large landslides under the action of reservoir water level rise and fall and rainfall. *Geol. Sci.Tech. Bull.* 40 (04), 153–161. doi:10.19509/j.cnki.dzkq.2021.0409

Tong, D. F., Tan, F., Su, A. J., Song, H. B., Lu, Z. C., and Yu, J. (2021). Evaluation of deformation mechanism and stability of Tanjiawan landslide based on multi-source data. *Geol. Sci.Tech. Bull.* 40 (04), 162–170. doi:10.19509/j.cnki.dzkq.2021.0432

Wang, G. L., Wu, F. Q., and Zhang, J. H. (2008). Rigid body element upper limit method for analysis and evaluation of heterogeneous soil slope stability. *J.Rock. Mech. Eng.* (2), 3425–3430.

Wang, X. D., Dai, F. C., and Huang, Z. Q. (2014). GIS Implementation of automatic search of the most dangerous sliding surface on reservoir bank slope Based on Swedish Strip method. *J.Rock. Mech. Eng.* 33 (S1), 3129–3134. doi:10.13722/j.cnki.jrme.2014.s1.075

Wang, Z. W., Zhao, F. R., Xie, W. P., and Lu, R. (2020). Analysis of formation conditionsand stability evaluation of gaojiawan landslide in Qinghai province. *W. Soil. Conserv. Bull.* 40 (03), 81–87. doi:10.13961/j.cnki.stbctb.2020.03.012

Wei, G., Yin, Z. Q., Shi, L. Q., Yuan, C. D., and Zhao, W. J. (2015). Analysis on development characteristics and stability of Linjiaya landslide in Beishan area of Xining City. *Geol. R.* 24 (02), 146–151. doi:10.13686/j.cnki.dzyzy.2015.02.012

Wu, L. L., Ke, Q., Lu, G., Zhang, J., Sun, L. N., and Jia, Y. Y. (2022). Research on the excavation stability evaluation method of Chaqishan ancient landslide in China. *Eng.Fail. Anal.* 141, 106664. doi:10.1016/j.engfailanal.2022.106664

Xiong, S., Yao, W. M., and Li, C. D. (2019). Stability evaluation of multilayer slopesconsidering runoff in the saturated zone under rainfall. *Eur. J. Environ. Civ. En.* 25, 1718–1732. doi:10.1080/19648189.2019.1600038

Yao, J., Li, X. Z., and Xu, R. C. (2021). Dynamic identification of potential landslide stability in a typical section of the proposed Sichuan-Tibet Railway under rainfall conditions. *J. D. Pete Mitigat. Eng.* 41 (03), 422–431. doi:10.13409/j.cnki.jdpme.202008015

Yao, S. H., Li, Z. M., and Zhang, J. Q. (2014). A study on the relationship between beishan landslide in xining and the fault in the north bank of Huangshui River. *Sci. Tech-Eng.* 14 (04), 161–163+169.

Zhang, J. C., Ma, T., Zhou, B., Wang, Z. F., Zhang, R., and Zhang, Y. Y. (2020). Seepage characteristics and stability analysis of old mudstone landslide under the action of rainfall: A case study of zhangjiacun landslide in huzhu county. *J. Qinghai Univ.* 38 (01), 87–92. doi:10.13901/j.carolcarrollnkiQHWXXBZK.01.014

Zhang, L. Y., and Zheng, Y. G. (2004). Extension of simplified Bishop method and its application to non-circular sliding surface. *Rock. Soil Mech.* (06), 927–929+934. doi:10.16285/j.rsm.2004.06.019

Zhang, X. D., Chen, J. P., Huang, R. Q., Yan, M., Lian, H. F., and Ding, H. J. (2003). FLAC-3D numerical simulation analysis of the stability of xiashan landslide. *Rock. Soil. Mech.* (1), 113–116. doi:10.16285/j.rsm.2003.s1.031

Zhang, Y., Xu, W. Y., Shi, C., Wang, R. B., and Sun, H. K. (2011). Three-dimensional numerical analysis of stability of large landslide accumulation body. *Rock. Soil. Mech.* 32 (11), 3487–3496. doi:10.16285/j.rsm.2011.11.042

Zhao, D. L. (1994). The hazards of mountain collapse and landslide in Xining City and their countermeasures. *Qinghai. Environ.* (01), 29–31+44.

Zhou, H. Q., Liu, D. S., and Chen, Z. H. (2008). Engineering analogy method and its application in landslide control engineering. *J. Und. Space. Eng.* 4 (06), 1056–1060.

Zhou, X. P., and Cheng, H. (2015). The long-term stability analysis of 3D creeping slopes using the displacement-based rigorous limit equilibrium method. *Eng. Geol.* 195, 292–300. doi:10.1016/j.enggeo.2015.06.002